International Journal of Heat and Mass Transfer 52 (2009) 5909–5921

Contents lists available at ScienceDirect

International Journal of Heat and Mass Transfer

journal homepage: www.elsevier.com/locate/ijhmt

Natural convection in a vertically divided square enclosure by a solid partition into air and water regions

Hakan F. Oztop, Yasin Varol *, Ahmet Koca

Department of Mechanical Education, Firat University, 23119 Elazig, Turkey

ARTICLE INFO

Article history:
Received 22 May 2009
Received in revised form 31 July 2009
Accepted 31 July 2009
Available online 7 September 2009

Keywords:
Natural convection
Heat transfer
Partition
Fluid

ABSTRACT

Numerical analyses of the flow and heat transfer due to buoyancy forces in a square enclosure divided by an impermeable partition between air and water filled chests were carried out using a finite difference technique. The enclosure was heated from left wall and cooled from right, isothermally. Horizontal walls were adiabatic. The partition divided the enclosure into air and water regions. Thus, two cases were examined: left side of partition was filled with air and right side was filled with water (Case I, air-partition-water) and left side was filled with water and right side with air (Case II, water-partition-air). Epoxy was chosen as partition material. Results were obtained for different Grashof numbers ($10^3 \leqslant Gr \leqslant 10^6$), thickness of the partition ($0.05 \leqslant \varepsilon \leqslant 0.2$) and location of the partition ($0.25 \leqslant c \leqslant 0.75$). An analytical treatment has been performed for low Grashof numbers. Numerical and analytical results gave an acceptable agreement. It was found that filling of fluid into chests is important for obtaining maximum heat transfer and energy saving. When left chest was filled with air (Case I), higher heat transfer was formed. It was an interesting result that heat transfer decreased with increasing of location of the partition for all values of partition thickness at Case I. On the contrary, heat transfer was a decreasing function of increasing value of location of the partition.

1. Introduction

Thermally driven flow and heat transfer in differentially heated enclosures have wide application areas in engineering such as solar collectors, double pane windows, fire spreads, etc. Wide and excellent reviews on these applications can be found in study of Ostrach [1], Catton [2], Gebhart et al. [3], De Vahl Davis and Jones [4]. The topic of these studies is mostly on natural convection in cavities bounded by solid walls with zero thickness.

A fully or partially dividers can be located inside the partitions to control heat transfer especially in electronical devices, nuclear reactors and building materials such as brick or some wall materials. Tong and Gerner [5] made a numerical study on natural convection in partitioned rectangular cavities with a vertical partition and filled with air and found that partitioning is an effective method of reducing heat transfer. Maximum reduction in heat transfer occurs when the partition is placed midway between the vertical walls. Turkoglu and Yucel [6] made a numerical study to investigate the conjugate natural convection in enclosures with vertical partitions. They searched the effects of number of partitions on natural convection and found that the mean Nusselt number decreases with increasing of partition number. Nishimura et al. [7] investigated the natural convection in enclosures with multiple vertical partitions both numerically and experimentally. They showed that the Nusselt number is inversely proportional to $(1 + N)$ where N is the number of partitions. They made a similar study using single partition by inserting off-center of the enclosure [8]. Ho and Yih [9] made a numerical study on conjugate natural convection in an air-filled rectangular cavity with a partition. Their study indicated that the heat transfer rate is considerably attenuated in a partitioned cavity in comparing with that for non-partitioned cavity. Acharya and Tsang [10] made a study on natural convection in inclined enclosures with a centrally located partition. Recently, Kahveci [11–13] investigated the natural convection in partitioned air filled enclosure using differential quadrature method. He found that average Nusselt number increases with decreasing of thermal resistance of the partition and partition thickness has little effect on heat transfer. Dzodzo et al. [14] investigated the effects of a heat conducting partition on the laminar natural convection heat transfer and fluid flow by comparing the numerical and experimental results for a cubic enclosure without and with a partition. The conclusion is that the introduction of a complete vertical partition reduces convective heat transfer from 59.1% to 63.6% in the range of Rayleigh numbers $38{,}000 < Ra < 369{,}000$. Neymark et al. [15] analyzed the phenomenon of natural convection of air and water in a partially

* Corresponding author. Tel.: +90 424 237 0000x4219; fax: +90 424 236 7064.
E-mail address: ysnvarol@gmail.com (Y. Varol).

0017-9310/$ - see front matter © 2009 Elsevier Ltd. All rights reserved.
doi:10.1016/j.ijheatmasstransfer.2009.07.016

Nomenclature

c	dimensionless location of the partition, c'/L
c'	location of partition in the x-direction, m
g	gravitational acceleration, m/s^2
Gr	Grashof number = $g\beta(T_h - T_c)L^3/\upsilon^2$
H	height of enclosure, m
k	thermal conductivity ratio = k_s/k_f
L	length of enclosure, m
Nu	local Nusselt number
$\overline{Nu}$	mean Nusselt number
Pr	Prandtl number = υ/α
T	temperature, K
u, v	dimensional velocities, m/s
U, V	non-dimensional velocities
X, Y	non-dimensional coordinates

Greek letters

ε	dimensionless thickness of the partition, ε'/L
ε'	thickness of the partition, m
υ	kinematic viscosity, m^2/s
θ	non-dimensional temperature = $(T - T_c)/(T_h - T_c)$
Ω	non-dimensional vorticity
β	thermal expansion coefficient, K^{-1}
α	thermal diffusivity, m^2/s
Ψ	non-dimensional stream function

Subscripts

A	air
s	solid
W	water
E	epoxy

Superscript

i	denotes left/right chest or partition

divided enclosure aiming to determine the effect of an internal partition on the natural convection in enclosures. Khan and Yaho [16] compared steady natural convection of water and air in a two dimensional, partially divided, rectangular enclosure. They indicated that flow configurations for air and water are completely different. Prandtl number has an important effect on the flow configuration. For the same Rayleigh number, geometry and boundary conditions, the average Nusselt number for water is about $2 \approx 5\%$ larger than that of air.

As listed above, there are many studies on partially divided enclosure. But there is no study on solid partition located between different fluid layers in systems. In this context, Nishimura et al. [17] performed a numerical work to analyze the natural convection in a rectangular enclosure horizontally divided into fluid and porous regions. Moshkin [18] used finite difference approximation of the Navier–Stokes equations under the Boussinesq-fluid assumption to simulate the flow and heat transfer in a two-layer system of an immiscible fluid. This problem also analyzed by different authors as Prakash and Koster [19,20], Richer [21], Richer and McKenzie [22], Dobretsov and Kyrdyashkin [23], Csereper and Rabinovich [24], Csereper et al. [25].

In this study, natural convection heat transfer was presented for a composite system as water-partition-air or air-partition-water in a differentially heated square cavity. In other words, thick solid partition was used to separate the fluid layers in the cavity. As an example, this case may be referred to cooling problem of internal combustion engines (one side filled with oil and other side cooling water), cooling of electronical heaters (air in one side and cooling fluid in other side) or solar collector (air in one side and phase change material to store heat in liquid phase in other side). Another example given by Mbaye and Bilgen [26] is that transient heat transfer in a composite passive system consisting of air-phase change material–air arranged as a rectangular enclosure. They studied geometrical and thermal parameters and found that subcooling coefficient was the most important parameter influencing heat transfer, and for a given subcooling, there was an optimum phase change partition thickness. To the best of the author's knowledge and from the above literature, there is a great lack of generalized information on natural convection in a divided enclosure filled with different fluids layers. Thus, the main aim of the present study is to investigate the natural convection fully divided with a partition in an enclosure filled with different fluid.

2. Physical model

Physical model is given in Fig. 1 with coordinates and boundary conditions. In this figure, cross-section of the cavity is square with $H = L$. It is heated from left vertical wall and cooled from right while top and bottom walls are adiabatic. The cavity is divided by a conductive partition with finite thickness ($\varepsilon = \varepsilon'/L$). Its material is chosen as epoxy due to its wide application in engineering. The location of the partition is given by $c = c'/L$. Two cases were treated. The left rectangular cavity is filled with water and right one with air (Case I) and the left one with air and right one with water (Case II).

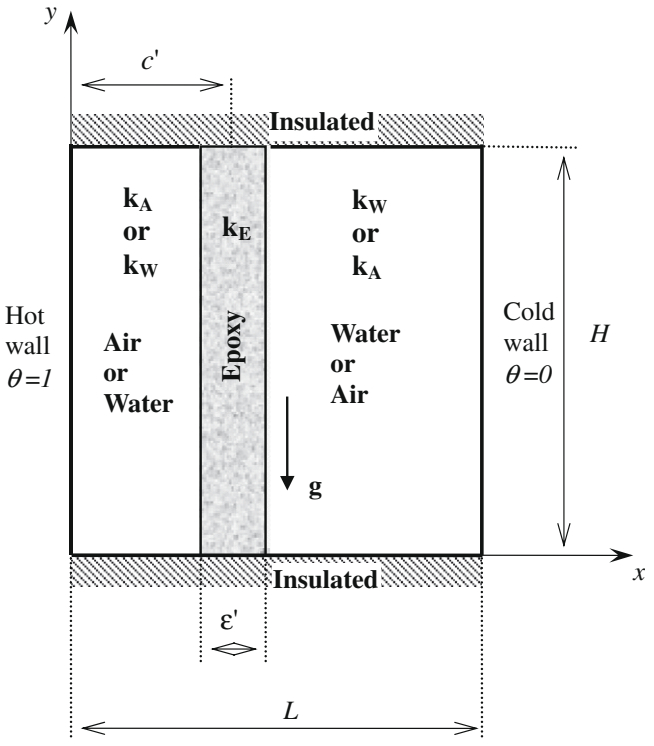

Fig. 1. Schematical configuration with coordinates and boundary conditions.

3. Governing equations

The system was considered to be laminar, incompressible and steady-state. The dimension perpendicular to the plane of the diagram is assumed to be long enough, so that the airflows may be conceived with 2-D motion. Dimensionless governing equation in vorticity–stream function formulation can be obtained by using the following dimensionless variables

$$X=\frac{x}{L},\quad Y=\frac{y}{L},\quad \Psi^i=\frac{\psi^i Pr^i}{\upsilon^i},\quad \Omega^i=\frac{\omega^i (L)^2 Pr^i}{\upsilon^i},$$
$$\theta=\frac{T-T_c}{T_h-T_c},\quad Pr^i=\frac{\upsilon^i}{\alpha^i},\quad u^i=\frac{\partial\psi^i}{\partial y},\quad v^i=-\frac{\partial\psi^i}{\partial x},$$
$$\omega^i=\left(\frac{\partial v^i}{\partial x}-\frac{\partial u^i}{\partial y}\right),\quad Gr=\frac{\beta^i g(T_h-T_c)L^3}{(\upsilon^i)^2} \tag{1}$$

The standard Boussinesq approximation adopted and all fluid properties are assumed to be constant. Based on the dimensionless variables above governing equations using vorticity–stream function formulation together with energy equation, the Navier–Stokes equations for a Newtonian fluid can be written in Eqs. (2)–(4). The equations have been scaled using the thermophysical properties of the right side.

$$-\Omega^i=\frac{\partial^2\Psi^i}{\partial X^2}+\frac{\partial^2\Psi^i}{\partial Y^2} \tag{2}$$
$$\frac{\partial^2\Omega^i}{\partial X^2}+\frac{\partial^2\Omega^i}{\partial Y^2}=\frac{1}{Pr^i}\left(\frac{\partial\Psi^i}{\partial Y}\frac{\partial\Omega^i}{\partial X}-\frac{\partial\Psi^i}{\partial X}\frac{\partial\Omega^i}{\partial Y}\right)-GrPr^i\left(\frac{\partial\theta^i}{\partial X}\right) \tag{3}$$
$$\frac{\partial^2\theta^i}{\partial X^2}+\frac{\partial^2\theta^i}{\partial Y^2}=\frac{\partial\Psi^i}{\partial Y}\frac{\partial\theta^i}{\partial X}-\frac{\partial\Psi^i}{\partial X}\frac{\partial\theta^i}{\partial Y} \tag{4}$$

For the solid region,

$$\frac{\partial^2\theta}{\partial X^2}+\frac{\partial^2\theta}{\partial Y^2}=0 \tag{5}$$

In above equations, [i = left chest and right chest]. A relatively higher Prandtl number was taken for partition. This approximation was taken from Moshkin [18] and Prakash and Koster [19]. Thus, left side of Grashof number was taken as base Grashof number.

3.1. Boundary conditions

It is assumed that walls of enclosures are solid and impermeable. Thus, all velocities and stream function are zero on the walls. The trapped air does not slip at the cavity walls. The temperature boundary conditions are established with a prescribed hot temperature T_h at the hot portion of the left vertical wall and a prescribed cold temperature T_c at the right vertical wall. On the other hand, the horizontal walls are adiabatic. Thus, the physical boundary conditions are illustrated in the physical model (Fig. 1) and they can be defined as follows:

$$\text{On the hot wall,}\quad U=V=0,\quad \theta=1,\quad \Omega=-\frac{\partial^2\Psi}{\partial X^2} \tag{6}$$

On the first interface ($X = c-\varepsilon/2$) and second interface ($X = c+\varepsilon/2$),

$$k\left.\frac{\partial\theta}{\partial X}\right|_s=\left.\frac{\partial\theta}{\partial X}\right|_f,\quad \Omega=-\frac{\partial^2\Psi}{\partial X^2} \tag{7}$$

where $k = k_s/k_f$ is the thermal conductivity ratio.

$$\text{On the cold wall,}\quad U=V=0,\quad \theta=0,\quad \Omega=-\frac{\partial^2\Psi}{\partial X^2} \tag{8}$$

$$\text{On adiabatic walls,}\quad U=V=0,\quad \partial\theta/\partial y=0,\quad \Omega=-\frac{\partial^2\Psi}{\partial Y^2} \tag{9}$$

The numerical method used in the present study is based on finite difference method to discretize the governing equations and the set of algebraic equations (Eqs. (2)–(9)) are solved using successive under-relaxation (SUR) technique. Thus, the velocity and temperature fields are obtained in the cavity. Regular grid was used for whole computational domain. Central difference method is applied for discretization of equations. The convergence criterion is chosen as 10^{-4} for all dependent variables and 0.1 is taken for under-relaxation parameter. A grid independence study is conducted using five different grid sizes of 31×31, 51×51, 81×81, 101×101 and 121×121. Regular grid was used for all cases. It is obtained that a further refinement of grids from 101×101 and 121×121 does not have a significant effect on the results in terms of average Nusselt number and stream function. According to this observation, a uniform grid size of 101×101 is enough for this study.

3.2. Heat transfer relations

The local and mean Nusselt numbers can be defined as follows:

$$\text{On hot wall}\quad Nu=\left.\frac{\partial\theta}{\partial X}\right|_{X=0}\quad\text{(heated wall)} \tag{10}$$

$$\text{On cold wall}\quad Nu=\left.\frac{\partial\theta}{\partial X}\right|_{X=c+\varepsilon/2}\quad\text{(right side of the partition)} \tag{11}$$

and mean Nusselt number is given by

$$\overline{Nu}=\int_0^H Nu\cdot dy \tag{12}$$

The horizontal walls of the cavity are considered adiabatic. Then, the heat flux evacuated from the vertical heated left wall must be identical to that crossing the cavity at each vertical plane. For the active vertical walls in contact with air and water, the energy balance leads to

$$-k_A\int_0^1 Nu_A\cdot dY=-k_W\int_0^1 Nu_W\cdot dY \tag{13}$$

Then

$$k_A\overline{Nu_A}=k_W\overline{Nu_W} \tag{14}$$

For Case I: (air-partition-water); $\overline{Nu_A}=\overline{Nu_H}$ and $\overline{Nu_W}=\overline{Nu_C}$. The conservation of heat flux leads to $\overline{Nu_H}=\frac{k_W}{k_A}\overline{Nu_C}$. Based on ratio of thermal conductivities.Thus,

$$\frac{k_W}{k_A}=22.5 \tag{15}$$

Table 1
Comparison of the values of mean Nusselt number with the literature.

Gr	k	$\overline{Nu}$ (Sanchez et al. [27])	$\overline{Nu}$ (Kaminski and Prakash [28])	$\overline{Nu}$ (present)
10^5	5	2.078	2.08	2.187
10^5	25	3.49	3.42	3.394
10^6	5	2.80	2.87	2.741
10^6	25	5.91	5.89	5.815

Table 2
Analytical results for mean Nusselt numbers using Eqs. (20) and (21) for Case II at $\varepsilon = 0.2$.

c	$\overline{Nu_H}$	$\overline{Nu_C}$
0.25	0.065	1.477
0.50	0.101	2.283
0.75	0.223	5.023

Then,

For Case I, $\overline{Nu}_H = 22.5\overline{Nu}_C$ (16)

For Case II, $\overline{Nu}_H = \frac{1}{22.5}\overline{Nu}_C$ (17)

Eqs. (16) and (17) are used to test for energy balance.

3.3. Validation of numerical code

Validation of the present code was performed by two different study from available literature as Sanchez et al. [27] and Kaminski and Prakash [28] in authors' earlier work [29]. In their case, the cavity is filled with single viscous fluid and bounded by single or double walls with finite length and thermal conductivity. Comparison between these studies and our code was performed and results are listed in Table 1. As seen from the table, obtained results show good agreement with the literature. Thus, it is decided that the present code is valid for further calculations.

3.4. Analytical treatment

An analytical treatment has been performed to validate the results at low Grashof numbers ($Gr = 10^3$, for example). In this case,

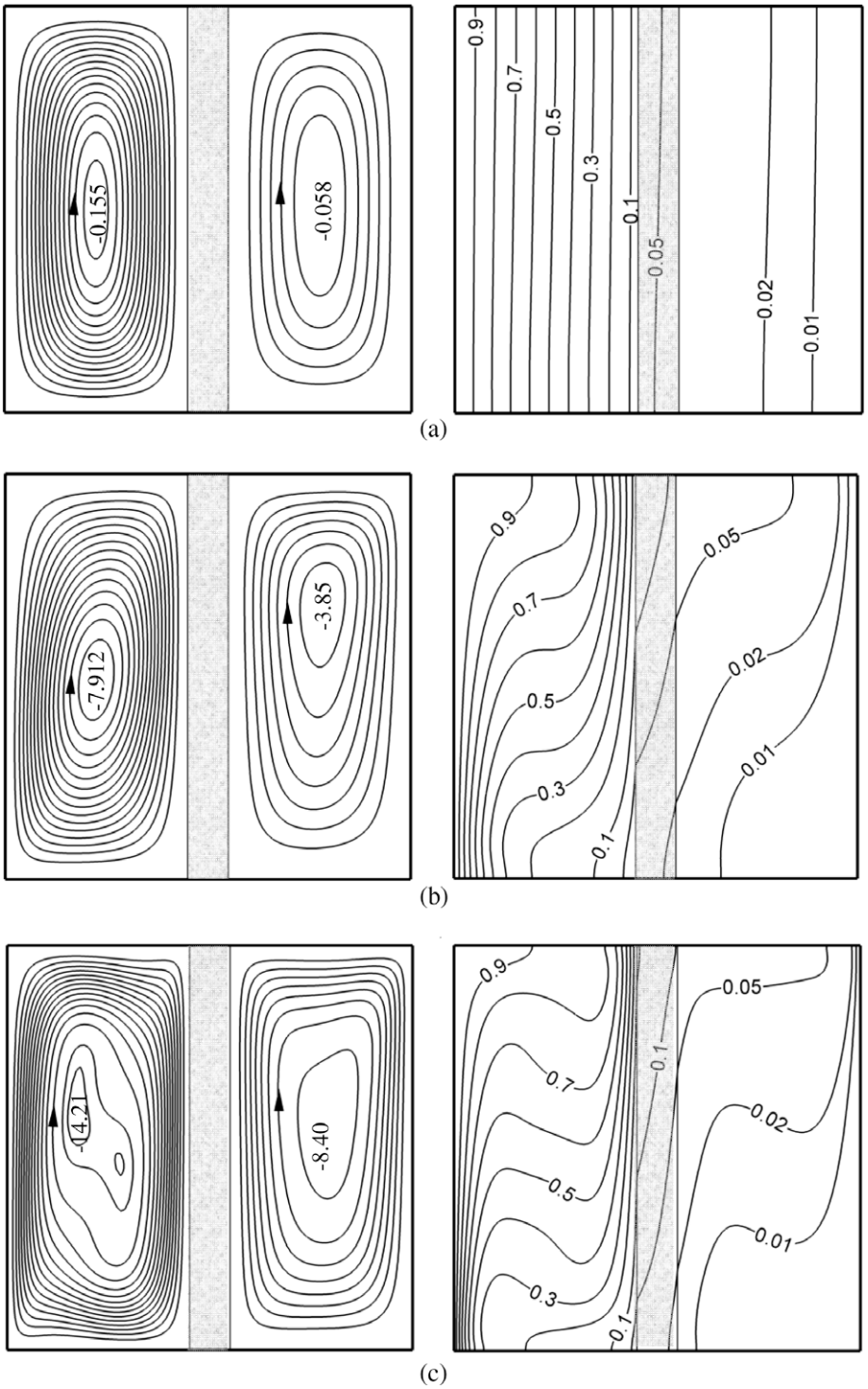

Fig. 2. Streamlines (on the left) and isotherms (on the right) at different Grashof numbers for Case I, $\varepsilon = 0.1$, $c = 0.5$, (a) $Gr = 10^3$, (b) $Gr = 10^5$, (c) $Gr = 10^6$.

conduction is the dominating heat transfer mode across the cavity. For this case, the heat flux density crossing the cavity in the horizontal direction ($-x$-direction) can be calculated analytically by considering the thermal analogy (conductive thermal resistance notion) as follows:

$$Q = -k_W \overline{\left.\frac{\partial T}{\partial x}\right|_W} = \frac{T_H - T_C}{\frac{c'-\varepsilon'/2}{k_W} + \frac{\varepsilon'}{k_E} + \frac{L-c'-\varepsilon'/2}{k_A}} = -k_A \overline{\left.\frac{\partial T}{\partial x}\right|_A} \tag{18}$$

In dimensionless form,

$$Q = k_W \overline{Nu_H} = \frac{1}{\frac{c-\varepsilon/2}{k_W} + \frac{\varepsilon}{k_E} + \frac{1-c-\varepsilon/2}{k_A}} = k_A \overline{Nu_C} \tag{19}$$

It follows that

$$\overline{Nu_H} = \frac{1}{(c-\varepsilon/2) + \frac{k_W}{k_E}\varepsilon + \frac{k_W}{k_A}(1-c-\varepsilon/2)} \tag{20}$$

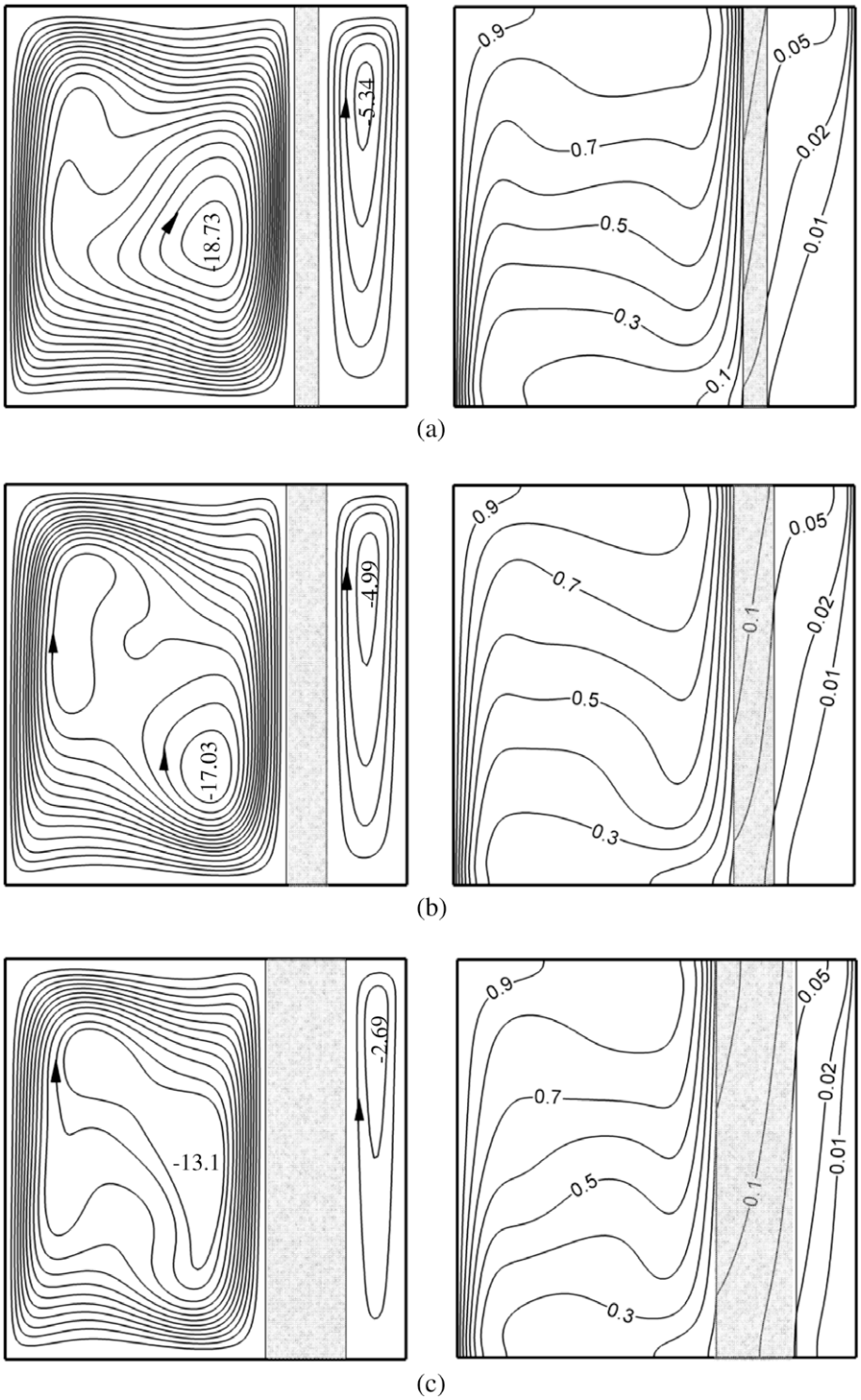

Fig. 3. Streamlines (on the left) and isotherms (on the right) at different thicknesses of partition for $c = 0.75$, Case I, $Gr = 10^5$, (a) $\varepsilon = 0.05$, (b) $\varepsilon = 0.1$, (c) $\varepsilon = 0.2$.

and

$$\overline{Nu_C} = \frac{1}{\frac{k_A}{k_W}(c-\varepsilon/2)+\frac{k_A}{k_E}\varepsilon+(1-c-\varepsilon/2)} \quad (21)$$

A test was performed for $\varepsilon = 0.2$ and results tabulated in Table 2. Values in the table and figures of mean Nusselt number for Case II (Figs. 10 and 11) are agree with each other. It means that numerical code gives acceptable results.

4. Results and discussion

A computational study has been performed to investigate natural convection in a square enclosure divided by solid partition into air and water regions. Computations were performed for different values of Grashof number, locations and thickness of the partition. The material of the partition is chosen as epoxy. The tests were performed for two cases: in the first case (Case I, air-partition-water), air is filled in left chest and water is filled in the right chest. In the second case (Case II, water-partition-air), the left chest is filled with water and the right one is air. Thus, the study focuses on the effects of location of fluids on heat transfer. We defined the dimensionless thermal conductivity ratio as $k = k_s/k_f$. Thus, dimensionless thermal conductivity is taken as $k = k_E/k_A = 9.9$ and $k = k_E/k_W = 0.44$, in Case I and Case II, respectively. Values of Prandtl number are 0.7 and 6.4 for air and water, respectively.

4.1. Results for Case I

Streamlines (on the left) and isotherms (on the right) are presented for $\varepsilon = 0.1$, $c = 0.5$ and different Grashof numbers in Fig. 2(a)–(c). The heated fluid moves from the hot wall and impinges to the top and top side of the partition. And then, it impinges to the bottom wall. Thus, it circulates in clockwise direction. As seen from the figure that single circulation cell was formed on both sides of the partitions but the strength of the fluid is lower at the right chest than that of left chest. For $Gr = 10^3$, the circulation is so weak due to domination of conduction mode of heat transfer as plotted in Fig. 2(a). Isotherms are also parallel to the vertical walls at this value of Grashof number. There is a huge temperature difference between two sides due to difference of Prandtl number of the fluids (Fig. 2b). The figure shows that the flow strength increases with increasing of Grashof number in both chests and isotherms deviate from the parallel structure. All figures show that circulation intensity is higher in the air filled chest due to domination of convection. Fluid temperature inside the water is extremely low due to weak transportation of heat from left side to right. It stems from low conductivity of air and the presence of epoxy partition. Here, the partition behaves as a curtain for heat transport. It will be seen from Nusselt number in next parts of the paper. For the highest values of Grashof number, the shape of the left chest is changed due to increasing of domination of convection mode of heat transfer. It also similar to the benchmark study

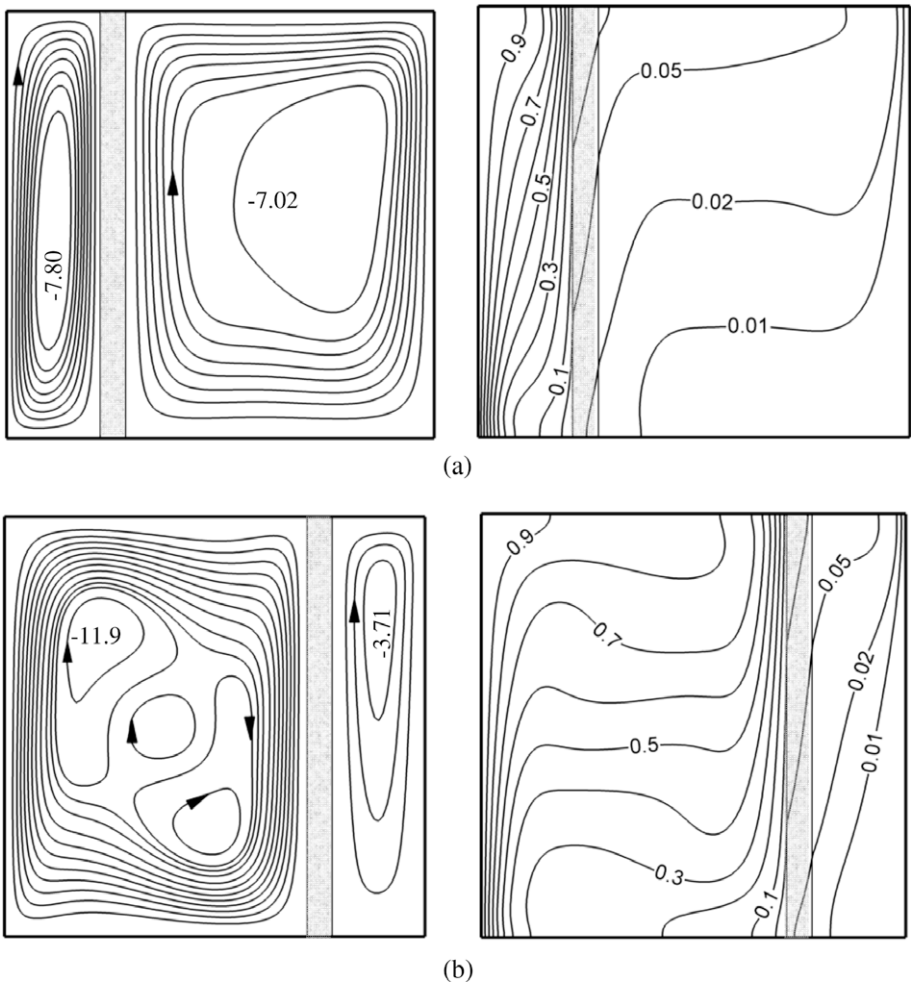

Fig. 4. Streamlines (on the left) and isotherms (on the right) at different locations of partition for $\varepsilon = 0.05$, Case I, $Gr = 10^6$, (a) $c = 0.25$, (b) $c = 0.75$.

of differentially heated cavity at $Gr = 10^6$ (Fig. 2(c)) which can be compared with De Vahl Davis and Jones [4]. In this case, flow strength increases in both chest and isotherms are almost parallel to the horizontal wall at the middle of the enclosure.

Fig. 3(a)–(c) shows the effects of partition thickness on streamlines (on the left) and isotherms (on the right) for $c = 0.75$ and $Gr = 10^5$ for Case I. Effects of partition thickness are tested from $\varepsilon = 0.05$ to $\varepsilon = 0.2$ in this figure. In this case, the right chest of the enclosure becomes shallower with increasing of partition thickness. Thus, the flow circulation path becomes almost same. As seen from the figure, egg shaped cell center was formed at the left chest but the main cell is elongated in $-y$-direction at the right with $\Psi_{min} = -5.34$ (Fig. 3a). Streamlines form a nearly centrally located single cell. There is a huge difference on flow intensity between two sides. The study of Kahveci [12], which is performed for a cavity with divided a partition filled same fluid, there is no big difference on flow intensity on both sides. Conduction heat transfer is dominant at the right chest (water filled side) even for the small partition thickness. For higher partition thickness, the top side of the partition is more heated when it is compared to the thin partition. Isotherms show that effectiveness of the convection mode of heat transfer increases with increasing of partition thickness at the air side. For the highest value of the partition thickness, the temperature of the fluid at right chest is almost equal to temperature of the right vertical wall.

Fig. 4(a) and (b) show the effects of location of the partition on flow fields and temperature distribution for $\varepsilon = 0.05$ and $Gr = 10^6$. For this value of Grashof number, as a consequence of increasing convective motion, temperature gradients near the heated wall becomes more severe. We presented the results for locations of the partition as $c = 0.25$ (near the hot wall) and $c = 0.75$ (near the cold wall). As illustrated from the figure, a main cell elongates through the vertical wall at the left chest and a circle shaped circulation cell was formed at the right chest. In this case, flow strength is higher

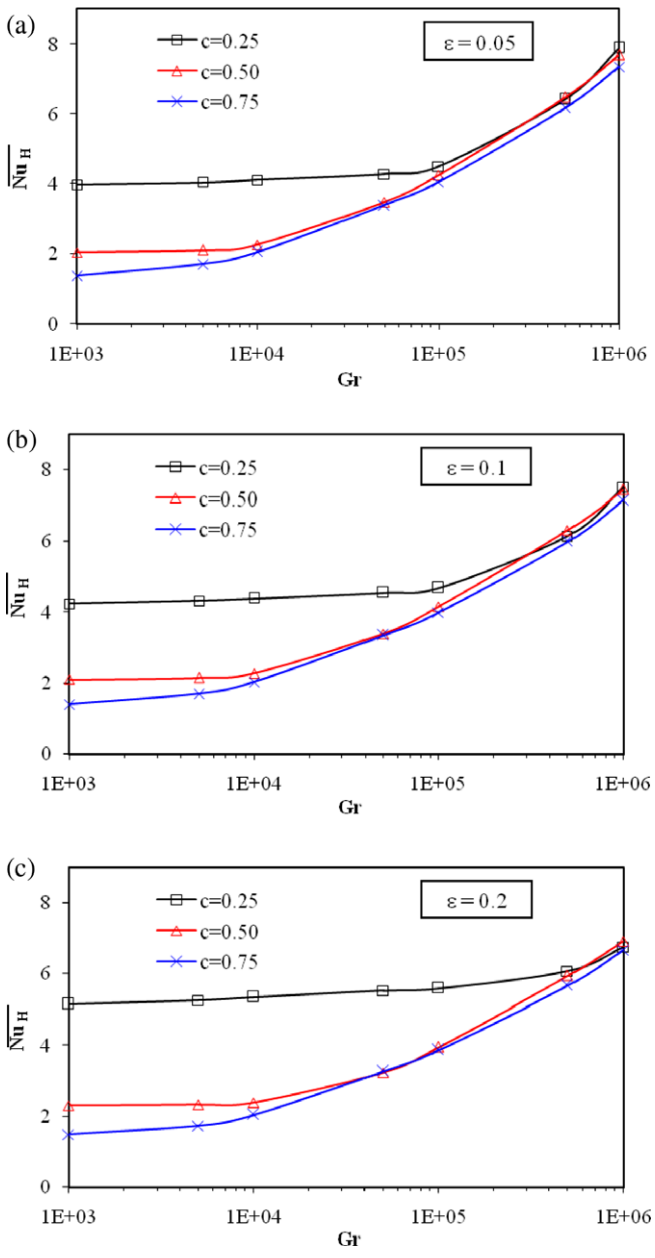

Fig. 5. Variation of mean Nusselt number with Grashof number at different locations of partition for hot side, Case I, (a) $\varepsilon = 0.05$, (b) $\varepsilon = 0.1$, (c) $\varepsilon = 0.2$.

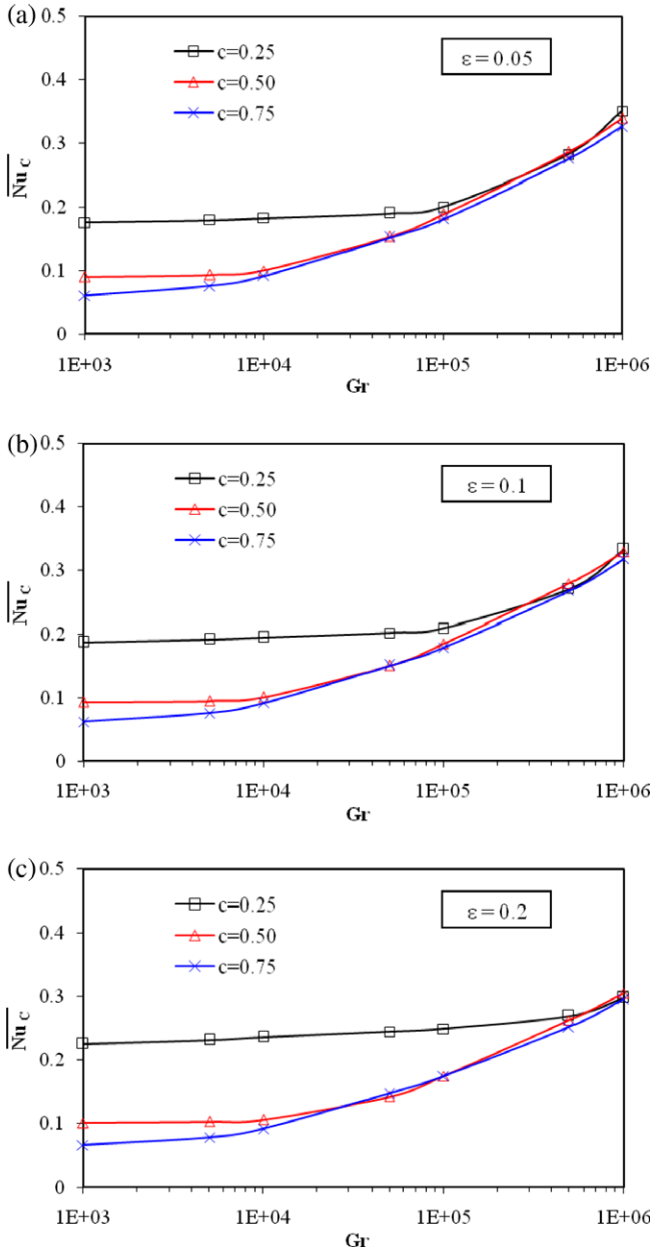

Fig. 6. Variation of mean Nusselt number with Grashof number at different locations of partition for cold side, Case I, (a) $\varepsilon = 0.05$, (b) $\varepsilon = 0.1$, (c) $\varepsilon = 0.2$.

at the right than that of right. Still, there is a huge difference in temperature at both sides due to presence of the partition. When the partition moves to the right wall, again, flow strength increases at the left chest. The figure can be compared with Fig. 3 to see the effects of Grashof number.

Variation of mean Nusselt number with Grashof number for both left and right side of the partition are presented in Figs. 5 and 6, respectively. Fig. 5(a) shows mean Nusselt numbers for $\varepsilon = 0.05$ and different locations of the partition. The mean Nusselt numbers were calculated from the left side of the partition using Eq. (12). As seen from the figure, conduction mode of heat transfer is dominant up to 8×10^4 and convection is effective over that value for $c = 0.25$. Thus, mean Nusselt number is constant up to this value. The lowest Nusselt number occurs for $c = 0.75$. The figure indicates that mean Nusselt numbers are decreased with increasing of location of the partition. Overall evaluation of Fig. 5 shows that heat transfer is an increasing function of wall thicknesses. Finally, results are showed that in high Grashof numbers range a boundary layer is established on the hot wall and convection mechanism becomes dominant. Fig. 6 shows the mean Nusselt

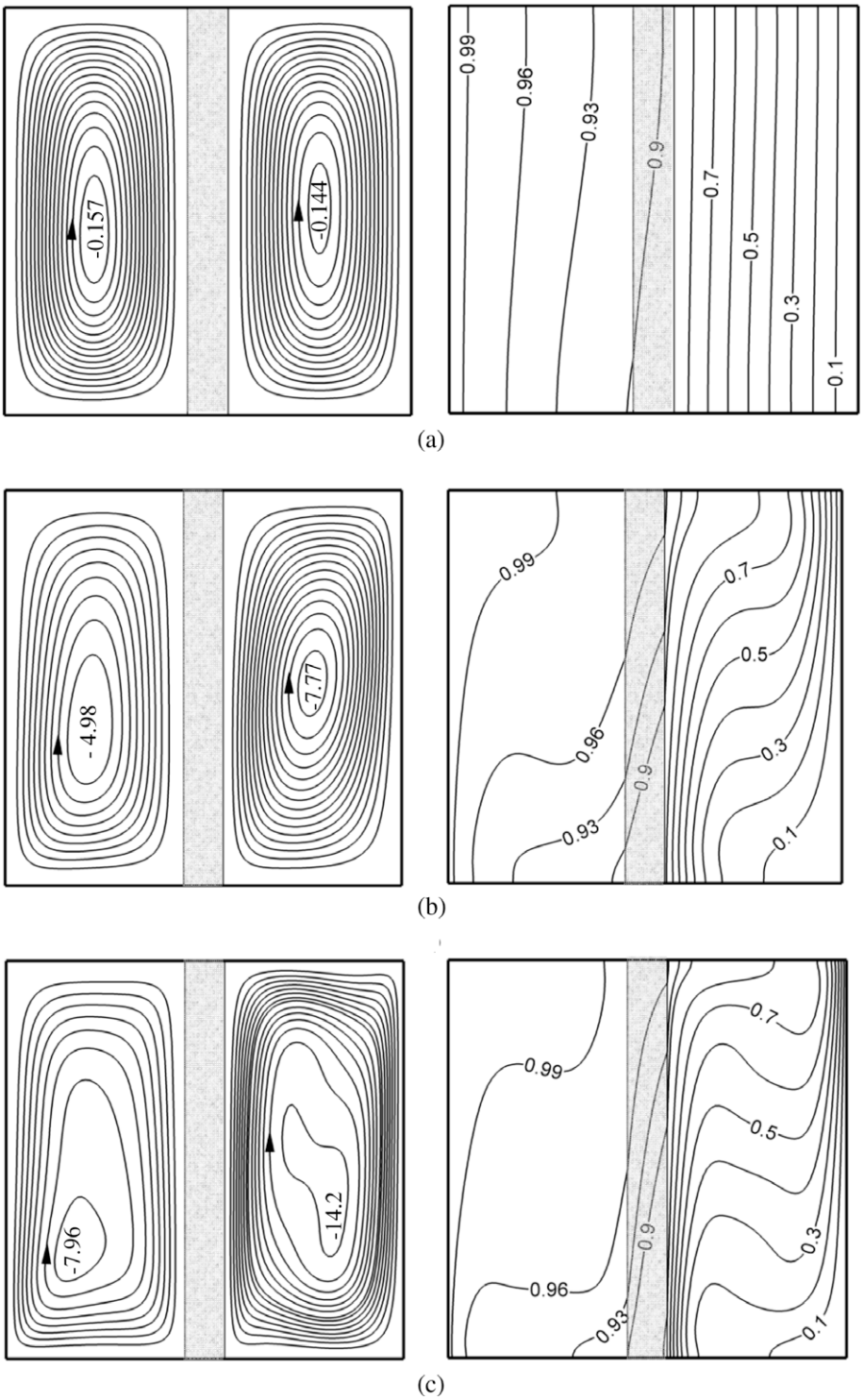

Fig. 7. Streamlines (on the left) and isotherms (on the right) at different Grashof numbers for Case II, $\varepsilon = 0.1$, $c = 0.5$, (a) $Gr = 10^3$, (b) $Gr = 10^5$, (c) $Gr = 10^6$.

numbers at the right side of the partition again for different partition thickness and location of the partition. As seen from the figures that values of mean Nusselt numbers are lower at the right side than that of left side.

4.2. Results for Case II

As indicated in previous part that the left chest of the enclosure is filled with water and the right one is air in Case II. Thus, a numerical solution comparing steady natural convection of different fluids filled at different chests is presented. Fig. 7 shows the streamlines (on the left) and isotherms (on the right) for $\varepsilon = 0.1$ and $c = 0.5$ at different Grashof numbers. As seen from the figure that again single circulation cell was formed in direction of clockwise rotation. Their values of stream function are close to each other as $\Psi_{min} = -0.157$ and $\Psi_{min} = -0.144$, on the left and right chest, respectively. In other words, there is no huge difference between flow intensity in both sides on the contrary of Case I. The temperature on water side is

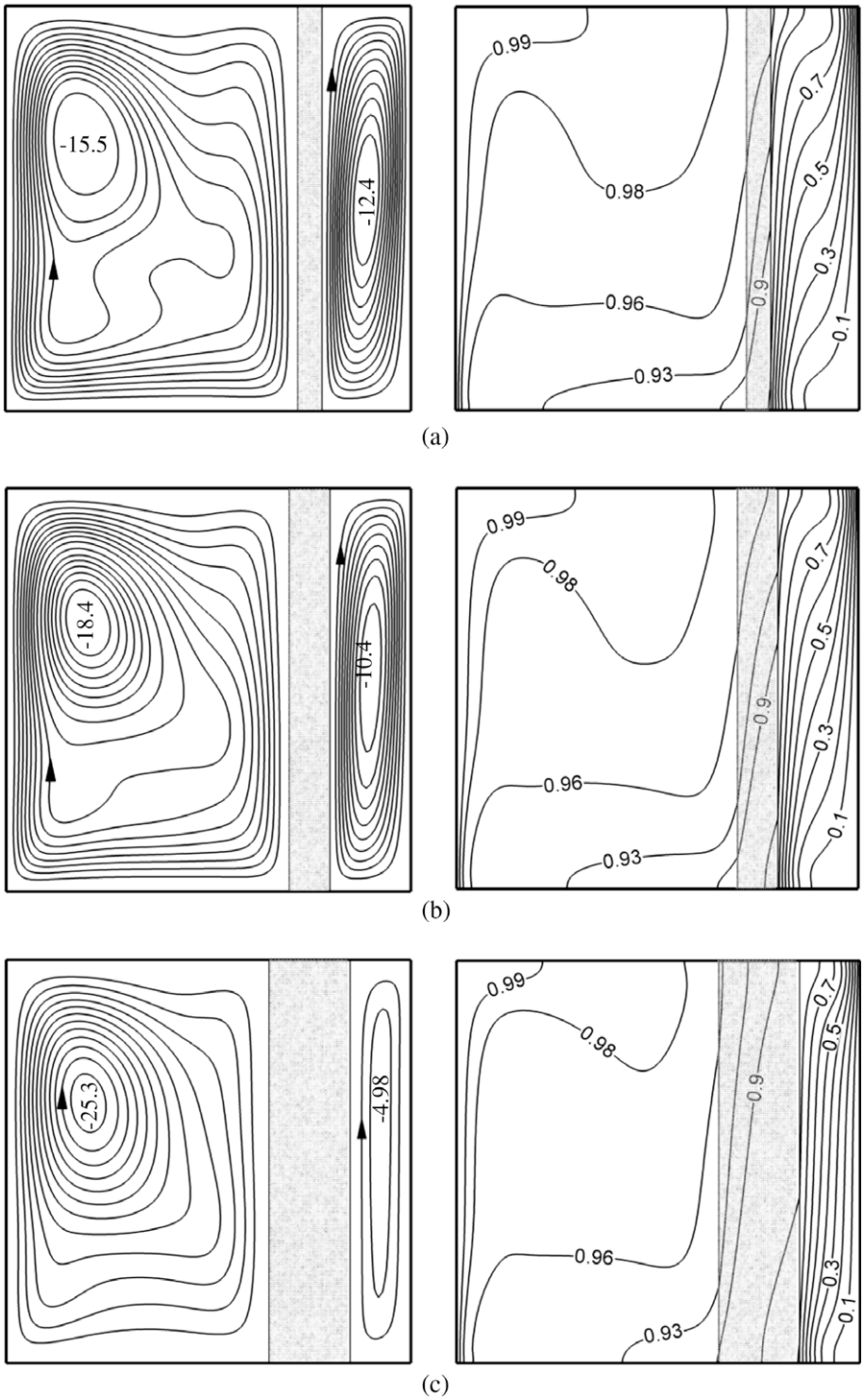

Fig. 8. Streamlines (on the left) and isotherms (on the right) at different thicknesses of partition for $c = 0.75$, Case II, $Gr = 10^5$, (a) $\varepsilon = 0.05$, (b) $\varepsilon = 0.1$, (c) $\varepsilon = 0.2$.

almost equal but it decreases from left to right inside the air side. It is due to the fact that domination of conduction for $Gr = 10^3$. Flow strength increases with increasing of Grashof number; however, temperature difference at the water side was still low even at the highest value of Grashof numbers. But differences on stream function values are increased with the increasing of Grashof numbers between two sides. On the contrary, the convection plays important role in the right chest due to low values of Prandtl number of air. As indicated by Khan and Yao [16] that Prandtl number has an important effect on the flow configuration. The effects of partition thickness on flow fields and temperature distribution are given in Fig. 8(a–c) by plotting the streamlines and isotherms patterns at $c = 0.75$ and $Gr = 10^5$. An oval shaped cell center was formed near the right bottom corner of the left chest. It becomes bigger and moves to the middle of the left chest with increasing of partition thickness. The flow strength values are higher for Case II than that of Case I at the left chest. On the contrary, they become smaller at the right chest. The flow and temperature distribution shows the same behavior with shallow cavities but temperature of the flow decreases due to presence of the partition. The skewness of isotherms is decreased with increasing of partition thickness. Fig. 9 shows the streamlines and isotherms for different locations of the partition. As given in the figure that when partition locates near the left vertical wall as $c = 0.25$, the flow strength decreases due to increasing of conduction mode of heat transfer. Both partition temperature and temperature of the air side decrease with the increasing of location of the partition.

Figs. 10 and 11 present the variation of mean Nusselt numbers with Grashof number for hot side and cold side of enclosure, respectively. It is clear from the Fig. 10 that heat transfer decreases when partition locates near the hot wall. Higher heat transfer was formed for higher value of c value. However, higher heat transfer was formed for higher partition thickness. Fig. 12 shows the comparison of velocity profiles for Case I (on the left column) and Case II (on the right column) at the mid-section in vertical way for different thickness of the partition at $c = 0.5$, $Gr = 10^3$ (Fig. 12a) and $Gr = 10^5$ (Fig. 12b). Velocity profile for Case I indicates that lower velocity is obtained for higher thickness of the partition at the left chest. On the contrary, fluid is motionless due to low Grashof numbers and domination of the conduction mode of heat transfer. In Case II, flow velocity is almost equal in each chest for $Gr = 10^3$ due to higher thermal conductivity of water which is filled at the left chest. For $Gr = 10^5$, velocity values are increased at the air side in both cases due to strong convection. It is an interesting result that lower velocity was formed in water filled chest.

Fig. 13 displays the temperature profiles for Case I (black lines) and Case II (red lines) at the mid-section of the cavity for different thickness of the partition at $c = 0.5$ and different Grashof numbers as $Gr = 10^3$ (Fig. 13(a)) and $Gr = 10^5$ (Fig. 13(b)). Firstly, it is noticed that higher temperature values are obtained in Case II than Case I. As seen from the figure, temperature is linearly decreased up to partition in an angle. Then, inclination angle changes after partition. Thickness of the partition makes small effect on temperature

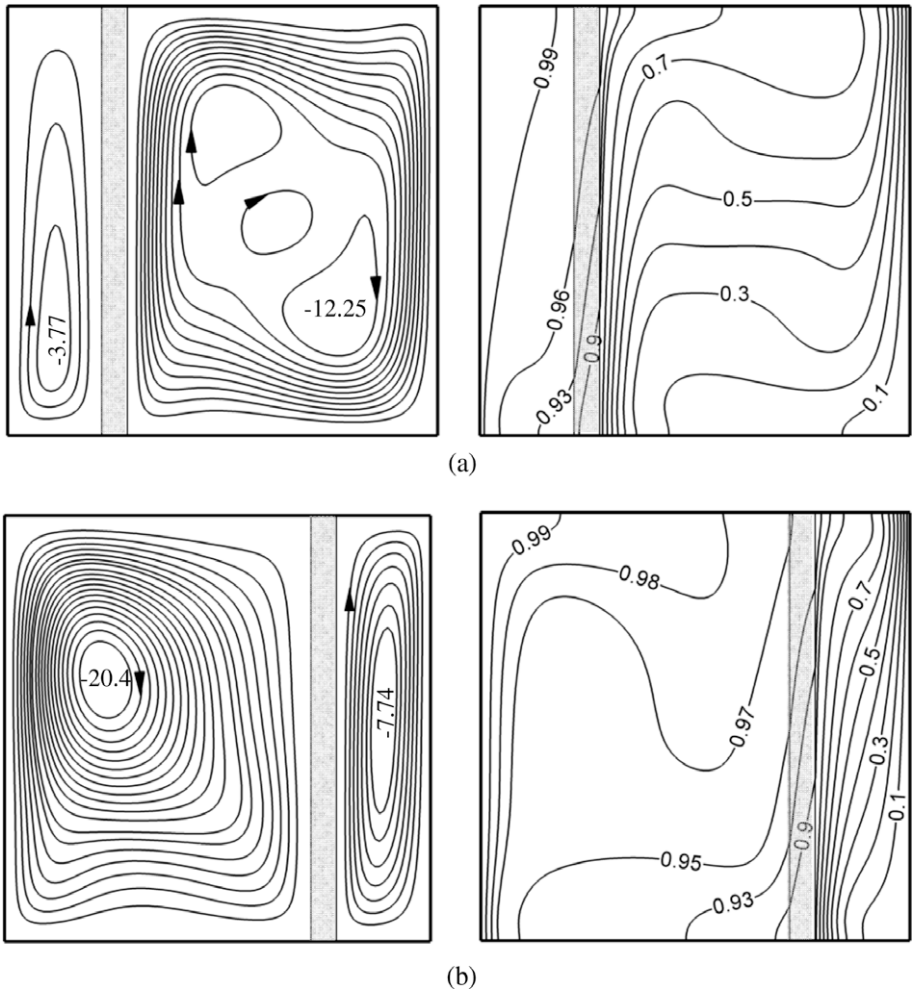

Fig. 9. Streamlines (on the left) and isotherms (on the right) at different locations of partition for $\varepsilon = 0.05$, Case II, $Gr = 10^6$, (a) $c = 0.25$, (b) $c = 0.75$.

profile in both cases for low Grashof numbers. Again, there is a decreasing along the x-direction of the enclosure for higher Grashof numbers. Wavy temperature profile was formed at the air side on both cases. On the contrary, temperature is linearly decreased at the water side due to low flow velocity as indicated earlier. Fig. 14 illustrates the temperature profiles for Case I (black lines) and Case II (red lines) at the mid-section in partition at $c = 0.5$ and different Grashof numbers as $Gr = 10^3$ (Fig. 14(a)) and $Gr = 10^5$ (Fig. 14(b)). As illustrated from the figure, temperature profile is constant along the partition for all values of partition thickness for Case I (Fig. 14(a)). For higher Grashof numbers as $Gr = 10^5$, heat transfer increases from bottom to top for both cases. Temperature value is decreased with increasing of partition thickness in Case II. On the contrary, effects of partition become insignificant in Case I.

Variation of local Nusselt number for Case I (black lines) and Case II (red lines) along the hot wall is presented in Fig. 15(a) and (b) for $Gr = 10^3$ and $Gr = 10^5$, respectively. The figures are plotted for different partition thicknesses and Grashof numbers and $c = 0.5$. As given in Fig. 15(a) local Nusselt number is decreased along the hot wall and it also decrease with increasing of partition thickness in Case I. On the contrary, it becomes constant around $Nu = 1.0$ in Case II. It means that location of different fluid in a system makes important effect even at small Grashof numbers. For higher Grashof numbers, local Nusselt number increases around the bottom hot wall, and then it decreases. Higher local Nusselt number values are formed in Case I than that of Case II. It is an interesting result that lower local Nusselt number is formed for higher partition thickness in Case I. On the contrary, higher local Nusselt value is obtained at higher partition thickness. This is due to the fact that depends on the thermal conductivities of the fluids in chests.

5. Conclusions

A numerical study was conducted to examine laminar natural convection flow fields and temperature distribution in a partially divided enclosure. The square cavity was with its vertical walls maintained at constant temperatures while its horizontal walls

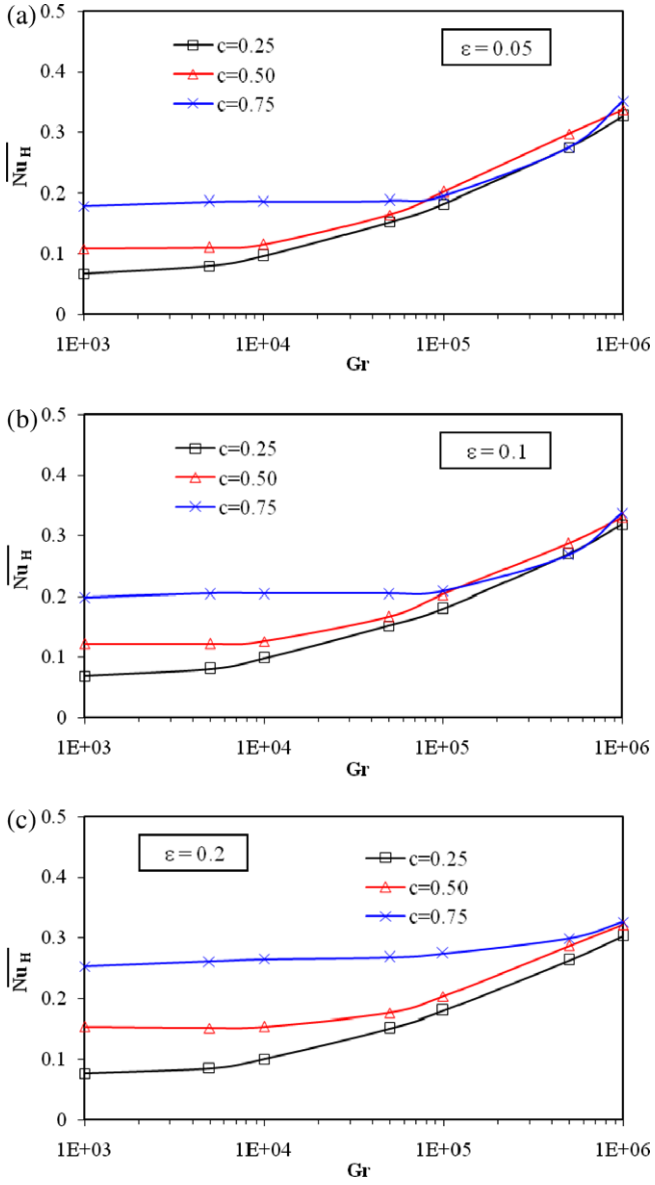

Fig. 10. Variation of mean Nusselt number with Grashof number at different locations of partition for hot side, Case II, (a) $\varepsilon = 0.05$, (b) $\varepsilon = 0.1$, (c) $\varepsilon = 0.2$.

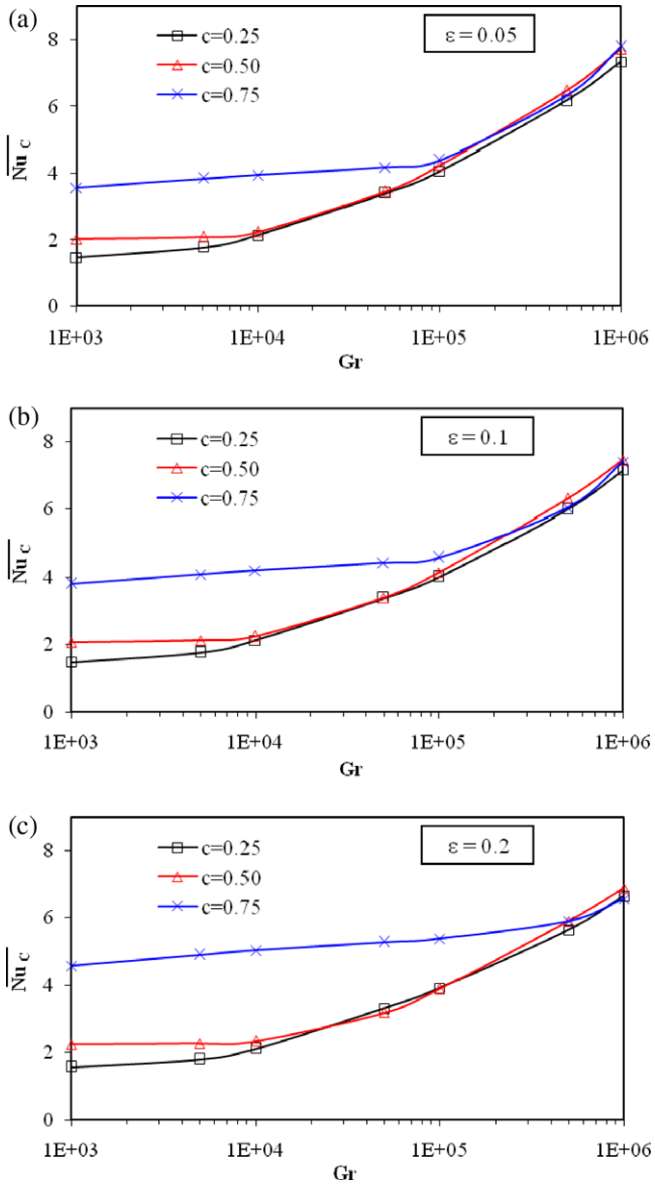

Fig. 11. Variation of mean Nusselt number with Grashof number at different locations of partition for cold side, Case II, (a) $\varepsilon = 0.05$, (b) $\varepsilon = 0.1$, (c) $\varepsilon = 0.2$.

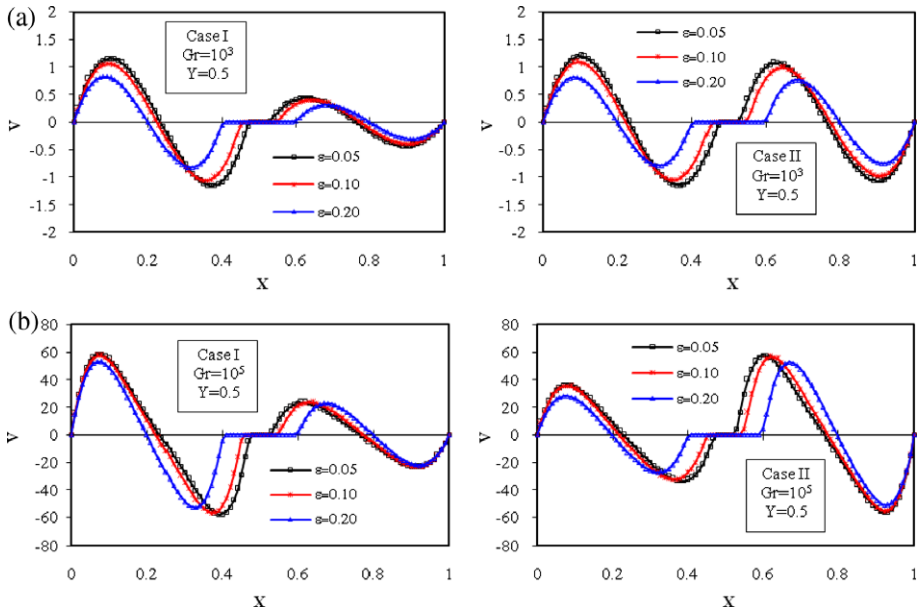

Fig. 12. Comparison of velocity profiles for Case I (on the left) and Case II (on the right) at the mid-section in vertical way for different thicknesses of the partition at $c = 0.5$ (a) $Gr = 10^3$, (b) $Gr = 10^5$.

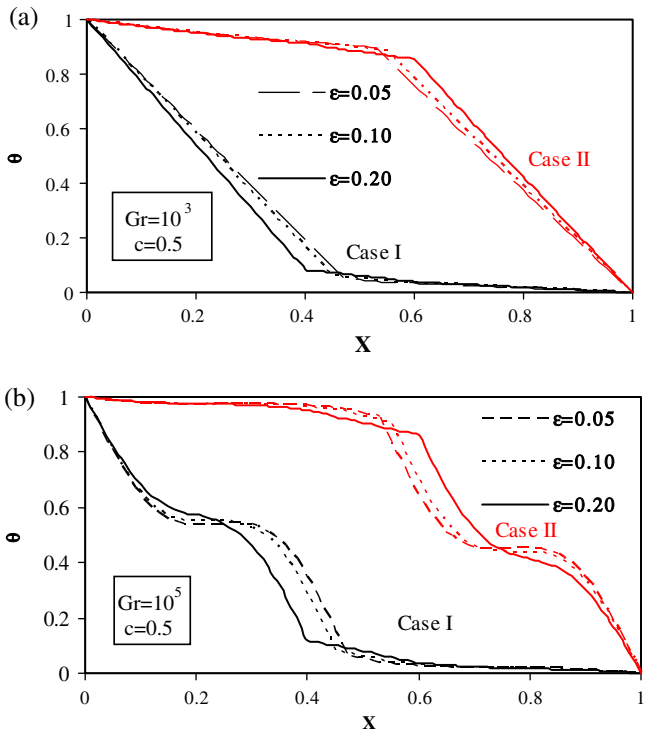

Fig. 13. Comparison of temperature profiles for Case I (black lines) and Case II (red lines) at the mid-section of the cavity for different thicknesses of the partition at $c = 0.5$ (a) $Gr = 10^3$, (b) $Gr = 10^5$. (For interpretation of the references to color in this figure legend, the reader is referred to the web version of this paper.)

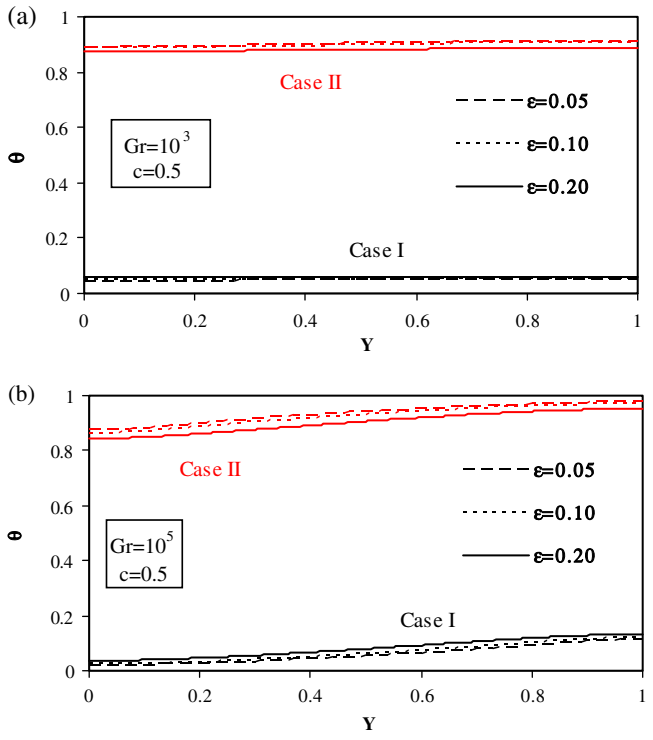

Fig. 14. Comparison of temperature profiles for Case I (black lines) and Case II (red lines) at the mid-section in partition for different thicknesses of the partition at $c = 0.5$ (a) $Gr = 10^3$, (b) $Gr = 10^5$. (For interpretation of the references to color in this figure legend, the reader is referred to the web version of this paper.)

insulated. The thick partition divided the enclosure into two different chests. Each chest was filled with different fluids such as water or air. The study was performed covering a range of parameters including Grashof number, Gr, location of the partition, c, and thickness of the partition, ε.

It is found that flow field, temperature distribution and heat transfer were affected from the changing of filled fluid in chests. When left chest was filled with air (Case I), higher heat transfer was formed. It was an interesting result that heat transfer decreased with increasing of location of the partition for all values of partition thickness at Case I. On the contrary, heat transfer was a decreasing function of increasing value of location of the partition. Heat transfer was a function of Grashof number that conduction mode of heat transfer became dominant at low

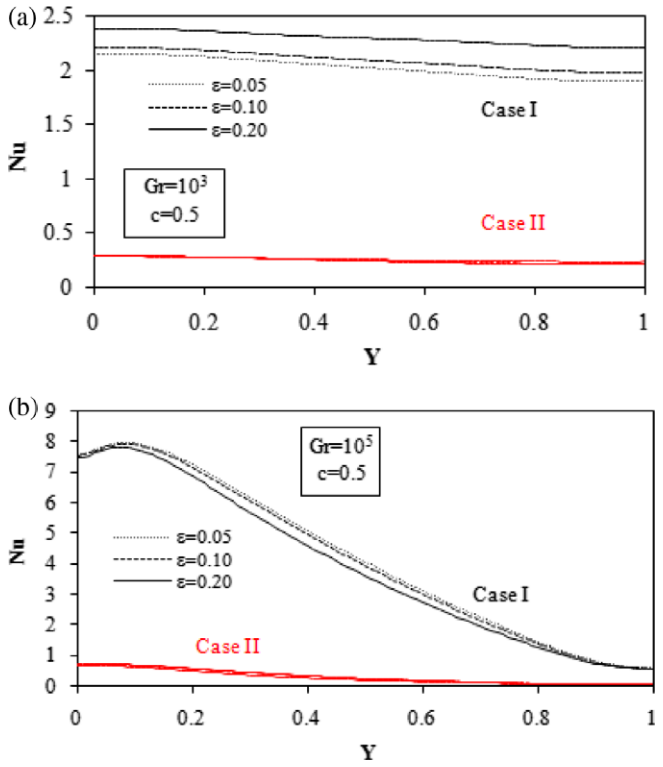

Fig. 15. Variation of local Nusselt number for Case I (black lines) and Case II (red lines) along the hot wall for different thicknesses of the partition at $c = 0.5$ (a) $Gr = 10^3$, (b) $Gr = 10^5$. (For interpretation of the references to color in this figure legend, the reader is referred to the web version of this paper.)

Grashof numbers especially partition was located near the hot wall.

References

[1] S. Ostrach, Natural convection in enclosures, J. Heat Transfer 110 (1998) 1175–1190.
[2] Catton, Natural convection in enclosures, in: Proc. Sixth Int. Heat Tr. Conf., vol. 6, 1978, pp. 13–31.
[3] B. Gebhart, Y. Jaluria, R.P. Mahajan, B. Sammakia, Buoyancy-Induced Flows and Transport, Hemisphere Publishing Corp., New York, 1988.
[4] G. De Vahl Davis, I.P. Jones, Natural convection in a square cavity: a bench mark numerical solution, Int. J. Numer. Methods Fluids 3 (1983) 227–248.
[5] T.W. Tong, F.M. Gerner, Natural convection in partitioned air-filled rectangular enclosures, Int. Commun. Heat Mass Transfer 13 (1986) 99–108.
[6] H. Turkoglu, N. Yucel, Natural convection heat transfer in enclosures with conducting multiple partitions and side walls, Heat Mass Transfer 32 (1996) 1–8.
[7] T. Nishimura, M. Shiraishi, F. Nagasawa, Y. Kawamura, Natural convection heat transfer in enclosures with multiple vertical partitions, Int. J. Heat Mass Transfer 31 (1988) 1679–1686.
[8] T. Nishimura, M. Shiraishi, Y. Kawamura, Natural convection heat transfer in enclosures with an off-center partition, Int. J. Heat Mass Transfer 30 (1987) 1756–1758.
[9] C.J. Ho, Y.L. Yih, Conjugate natural heat transfer in an air-filled rectangular cavity, Int. Commun. Heat Mass Transfer 14 (1987) 91–100.
[10] S. Acharya, C.H. Tsang, Natural convection heat transfer in a fully partitioned inclined enclosure, Numer. Heat Transfer 8 (1985) 407–428.
[11] K. Kahveci, Natural convection in a partitioned vertical enclosure heated with a uniform heat flux, J. Heat Transfer 129 (2007) 717–726.
[12] K. Kahveci, A differential quadrature solution of natural convection in an enclosure with a finite-thickness partition, Numer. Heat Trans. A 52 (2007) 1009–1026.
[13] K. Kahveci, Numerical simulation of natural convection in a partitioned enclosure using PDQ method, Int. J. Numer. Methods Heat Fluid Flow 17 (2007) 439–456.
[14] D.M.C. Dzodzo, M.B. Dzodzo, M.D. Pavlovic, Laminar natural convection in a fully partitioned enclosure containing fluid with nonlinear thermophysical properties, Int. J. Heat Mass Transfer 20 (1999) 614–623.
[15] J. Neymark, C.R. Boardman, A. Kirkpatrick, High Rayleigh number natural convection in partially divided air and water filled enclosure, Int. J. Heat Mass Transfer 32 (1989) 1671–1679.
[16] J.A. Khan, G.F. Yao, Comparison of natural convection of water and air in a partitioned rectangular enclosure, Int. J. Heat Mass Transfer 36 (1993) 3107–3117.
[17] T. Nishimura, T. Takumi, M. Shiraishi, Y. Kawamura, H. Ozoe, Numerical analysis of natural convection in a rectangular enclosure horizontally divided into fluid and porous regions, Int. J. Heat Mass Transfer 29 (1986) 889–898.
[18] N.P. Moshkin, Numerical model to study natural convection in a rectangular enclosure filled with two immiscible fluids, Int. J. Heat Fluid Flow 23 (2002) 373–379.
[19] A. Prakash, J.N. Koster, Steady natural convection in a two-layer system of immiscible liquids, Int. J. Heat Mass Transfer 40 (1997) 2799–2812.
[20] A. Prakash, J.N. Koster, Steady Rayleigh–Bénard convection in a two-layer system of immiscible liquids, J. Heat Transfer 118 (1996) 366–373.
[21] F.M. Richer, Focal mechanisms and seismic energy release of deep and intermediate earthquakes in the Tonga Kermadec region and their bearing on the depth extent on mantle flow, J. Geophys. Res. 84 (1979) 6783–6795.
[22] F.M. Richer, D.P. McKenzie, On some consequences an possible causes of layered mantle convection, J. Geophys. Res. 86 (1981) 5142–6135.
[23] N.L. Dobretsov, A.G. Kyrdyashkin, Structure of free-convection flows in a horizontal layer of liquid under various boundary conditions, Fluid Mech. Sov. Res. 9 (1990) 1–36.
[24] L. Csereper, M. Rabinovich, Gravity and convection in two-layer mantle, Earth Planet. Sci. Lett. 76 (1985) 193–207.
[25] L. Csereper, M. Rabinovich, C. Rosemberg-Borot, Three dimensional infinite Prandtl number convection in one and two-layers with applications for the Earth's gravity field, J. Geophys. Res. 93 (1988) 12009–12025.
[26] M. Mbaye, E. Bilgen, Natural convection in composite systems with phase change materials, Heat Mass Transfer 42 (2006) 636–644.
[27] F. Sanchez, F. Solorio, R. Avila, Conjugate natural convection in a square cavity heated from below, in: Proceedings of IMECE04, ASME Int. Mech. Eng. Congress and exposition, Anaheim, California, USA, 2004, pp. 1–10.
[28] D.A. Kaminski, C. Prakash, Conjugate natural convection in a square enclosure: effect of conduction in one of the vertical walls, Int. J. Heat Mass Transfer 29 (1986) 1979–1988.
[29] Y. Varol, H.F. Oztop, A. Koca, Entropy generation due to conjugate natural convection in enclosures bounded by vertical solid walls with different thicknesses, Int. Commun. Heat Mass Transfer 35 (2008) 648–656.